INTERNATIONAL JOURNAL OF AUTOMOTIVE SCIENCE AND TECHNOLOGY

2025, VOL. 9, NO: SI 1st Future of Vehicles, 12-21 www.ijastech.org e-ISSN: 2587-0963

Comparative Analysis of Aluminum and Steel Sheets in Lightweight Car Body Applications

Imre Czinege

Department of Materials Science and Technology, Széchenyi István University, H-9026 Győr, Hungary

Abstract

The use of lightweight materials in vehicle production is a key trend in the automotive industry, driven by a need for greater efficiency, sustainability and improved performance. Key materials include aluminum, magnesium and titanium alloys, as well as various types of advanced high-strength steel. Fiber-reinforced polymers (such as glass, carbon and aramid) are ideal for reducing weight, particularly in internal structures. This paper analyses the effect of weight reduction on energy consumption using up-to-date weight and energy consumption data for internal combustion engines and battery electric vehicles. To compare AlMg alloys and steels, a sheet-specific version of the Ashby concept was developed. This supplements the Material-Shape-Process characteristics with three additional parameter groups: Design Parameters, Formability Characteristics and Shape Constraints. Some of these material parameters were further analyzed using a banana chart constructed from a database collected in our own laboratory. This chart was then compared with other global and local formability parameters, such as the Forming Limit Diagram (FLD) and Erichsen number. It was concluded that these characteristics only follow the trend defined in the banana diagram to a limited extent, so complex parameter sets according to the extended Ashby concept were needed to characterize the complex forming process. A further comparison was conducted between aluminum and steel sheets using a multi-objective optimization method for strength and stiffness parameters.

Keywords: Ashby model; Banana diagram; Energy consumption; Lightweight materials; Material characterization; Multi-objective optimization; Strength-to-density function

Research Article

History
Received 31.07.2025
Revised 18.08.2025
Accepted 24.09.2025

Contact
* Corresponding author
Imre Czinege
czinege@sze.hu
Address: Department of Materials Science and Technology, Széchenyi István University, H-9026 Győr, Hungary
Tel: +36309008810

***To cite this paper*:** Czinege, I. Comparative Analysis of Aluminum and Steel Sheets in Lightweight Car Body Applications. International Journal of Automotive Science and Technology. 2025; 9 (SI 1st Future of Vehicles): 12-21. https://doi.org/10.30939/ijastech..1755417
*This article is part of a special issue entitled: '1st Future of Vehicles: Innovation, Engineering and Economic Conference'.

1. Introduction

Over the last few decades, the demands of car buyers have changed significantly. They now expect increased functionality, comfort and enhanced safety, while also aiming to reduce costs over the vehicle's service life.

However, the extended functionality and comfort demand significantly increase the weight of cars, which increase energy consumption and operational costs. Consequently, the conflicting objectives of achieving greater comfort and reducing fuel use have become the driving force behind the automotive industry's push towards lightweight vehicle design. The advantages of reducing weight are clear: lower fuel consumption, reduced CO_2 emissions and improved driving dynamics without the need for increased engine performance. However, increasing safety regulations present another challenge for car designers, as lightweight materials generally offer lower strength than steel, and their cost is sometimes higher. These aspects have motivated car manufacturers to develop advanced materials, new design methods and production techniques that can fulfil these complex demands.

Many authors advocate reducing CO_2 emissions by increasing the proportion of electric vehicles (BEVs) rather than internal combustion engine vehicles (ICEVs) [1]. However, it is also well established that reducing a vehicle's weight leads to lower fuel or energy consumption for both ICEVs and BEVs [2]. Publication [3] estimates a 5% reduction in fuel consumption and emissions when the weight of a vehicle is decreased by 15–20%. Various analyses on the internet support these findings: for instance, a 10% weight reduction generates a 6% improvement in fuel economy, and electric vehicles also experience an increase in driving range. However, this information is not supported by appropriate measurements and differs from the statement in [2]. Other sources state that reducing a vehicle's weight by 100 kg results in a 5 g/km decrease in CO_2 emissions.

There are also calculations regarding the relationship between weight and the energy consumption required to move the vehicle. These calculations estimate the average energy demand to be 0.8–1 kWh/100 km/100 kg. Despite known consumption growth data, the weight of cars increased significantly worldwide from 1985 to 2005. After this period, the growth rate decreased due to lightweighting efforts.

Vehicle weight can be reduced while maintaining safety requirements by developing higher strength grades of the same material, or by using lower-density materials with an equivalent or better specific strength (strength-to-density ratio) than the material to be replaced. Examples of the first solution include advanced high-strength steels (AHSS), while the second solution involves the use of lower-density, high-strength aluminium alloys. A possible classification of lightweight materials is summarised in [4]. The authors divide these materials into four categories: light metal alloys (e.g. aluminium, magnesium and titanium); the AHSS family (e.g. DP, TRIP and TWIP); polymer composites (e.g. carbon fibre reinforced plastics); and smart materials, which represent the future and are described in detail in publication [5].

These materials will only achieve the desired results if they are selected in conjunction with modern design methods. The development of design and material selection models is presented in publication [6] for the period between 1978 and 2010; naturally, this is not exhaustive. In this area, the research results of M. F. Ashby et al. [7-10] are outstanding; they summarised the complex design and material selection process in the material–shape–process triangle. These theoretical results have practical applications supported by the computer-aided design system integrated for example into Ansys. This system relies on a large database to help users make the best material choices in an interactive way. A good example can be found in [11]. Several authors have applied or further developed the Ashby model, some results can be found in publications [12-15].

The original Ashby concept aimed to optimise one parameter to minimise weight under various material properties and constraints [7]. Subsequently, the need arose for the development of multi-objective optimisation models, one possible solution to which was presented by Ashby in [8]. He also stated that several factors, such as cost, mass, volume, power-to-weight ratio and energy density, should be considered simultaneously in design. This also initiated further applications, examples of which can be found in references [16-21]. Multi-objective solutions that combine material selection and CO_2 emission reduction deserve special attention [22-25]. Extending this to the entire life cycle, the goal is for a systematic material selection process to integrate weight optimisation and environmental life cycle assessment [26].

Over the past 10 years, more studies have been published in the field of design and material selection that rely heavily on artificial intelligence (AI) tools. One such method is generative design [27-30]. Publication [31] analyses how artificial intelligence is transforming the design thinking process; publication [32] provides an overview of the further spread of AI; and publication [33] presents artificial neural network (ANN) methods focused on materials design and manufacturing.

Alongside the presented design and material selection concepts, significant development has also been shown in vehicle materials [4]. Many models have been produced with an all-aluminium body, with the 2015 Jaguar XE being a notable example. There are also positive results from using titanium and magnesium, but they are used less frequently in vehicle construction. Polymer composites are finding even wider application in the automotive industry, as detailed in publication [34]. According to the authors' analysis, weight savings of 16–55% can be achieved, depending on the components used. The BMW i3 model is the most well-known example of a composite body, with a weight reduction of 60% compared to steel and 40% compared to aluminium. However, recent development trends indicate an expansion of the multi-material concept. A detailed analysis of the assessment of suitable automotive component ranges for multi-material design can be found in [35]. Hybrid material pairings are also increasingly being used within a single component; the [5] publication highlights aluminium-steel, magnesium-aluminium, and CFRP-aluminium pairings.

Sheets are of paramount importance in car body construction, with steel and aluminium being the two most common materials. In the case of body steels, the two main parameters included in the well-known banana diagram [36-38] are strength and formability. This illustrates the trade-off between yield strength and ultimate tensile strength, as higher strength is usually coupled with lower formability. The banana diagram characterises the global formability parameters of sheets. Other local formability and diffuse necking test results are also important for design purposes and are summarised in [39]. However, to describe the complex process of sheet metal forming, additional strength parameters are needed, such as the flow stress curve and the yield surface. These can be determined based on various yield criteria. These material characteristics provide the basic parameters for various sheet metal forming design systems, such as AutoForm, LS-Dyna and PAM-STAMP. These models are analysed and summarised in Banabic's 2010 book [40], and [41] presents the latest developments up to 2020, for example.

Based on the wide range of applications for lightweighting, this study focuses on the sheet metals most frequently used in car body and chassis construction: steels and AlMg alloys. Section two presents the materials included in the study and describes an improved application of the well-known Ashby model for sheet forming. The third section, 'Results', examines three topics. Firstly, it focuses on the relationship between vehicle weight and energy use. This is followed by a material-specific analysis, comparing the strength and formability parameters of steel and aluminium sheets. The third topic concerns the application of multi-material optimisation to select appropriate car body materials. Section 4 summarises the results and conclusions.

2. Research Methods

This section includes a discussion of two topics. The first part describes the materials included in the studies and their test methods. The second subsection further develops the Material-Shape-Process system of the original Ashby concept in relation to sheet metal analysis.

2.1. Materials and testing methods

The materials and test results used in the various analyses were obtained from the Materials Testing Laboratory database at Széchenyi István University. These tests were conducted according to the requirements of automotive component manufacturers, using sheet metal supplied by them. The steel sheets tested were classified into the Mild Steel (MS) and Advanced High Strength Steel (AHSS) categories, namely dual phase (DP600, DP800, DP1000) and TRIP steels. Test specimens of aluminium alloys were selected from AlMg3 (AA5754) and AlMg4.5 (AA5182) grades. Magnesium alloys are represented by AZ31B and TiAl6 grades have also been added to the database. It should be noted that, among the AlMg alloys, both annealed (O) and hardened (H14, H22) sheets can be found; this results in significant scatter in the measured data. The same is true of DP600 samples, where the yield strength varies between 350 and 450 MPa.

Tensile tests were performed using a 100 kN capacity Instron 5582 tensile testing machine with a video extensometer for strain measurement. The extensometer measured longitudinal and transverse strain between two points. The specimens were cut according to the DIN EN 10002 standard; in most cases, the gauge length was 80 mm, and the width was 20 mm. The specimens were cut in three directions: 0°, 45° and 90° relative to the rolling direction. The test results were recorded and evaluated using Instron Bluehill 2 software. To better characterise the formability, Nakajima tests were also carried out and Forming Limit Diagrams (FLDs) were determined according to ISO 12004-2:2009 on three parallel specimens with seven different geometries per sheet material. Measurement and evaluation were performed using the GOM ARAMIS® hardware-software system. Further tests included cup drawing and Erichsen tests.

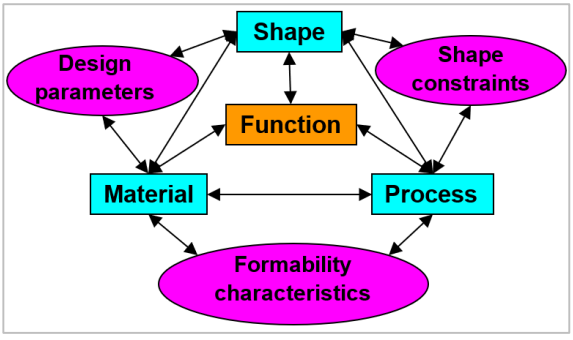

Figure 1. Extended Ashby model

2.2. Sheet metal specific model

The original Ashby concept defines the function of a component by its Material, Shape and Process parameters, as shown in Figure 1. For sheet metal analysis, this model can be specified with three additional databases: Design parameters, Formability characteristics, and Shape constraints. Data defined in this way creates relationships between the initial material, shape and process factors.

The Design parameters are located between material and shape in Figure 1 and contain the data necessary for dimensioning the part, e.g. yield strength, elastic modulus, fracture strength and fatigue limit. The design software used might be any integrated CAD system that includes a Finite Element Module (FEM) for strength and crash analysis. This ensures that the shape and its material parameters are harmonised and that both the geometric dimensions and the material selection fulfil the demands of the defined load and the component's constraints. Among the Formability characteristics, the first parameters to mention are those derived from the tensile test: uniform strain, total elongation, hardening exponent and anisotropy coefficient (r-value). Software used for complete process modelling might include AutoForm, LS-Dyna or PAM-STAMP. The input data for these is the flow stress curve (FSC), the forming limit diagram (FLD) and the yield surface (YS), as well as the friction coefficient specialised for the process. Finally, the shape constraints that characterise the relationship between shape and process include manufacturing constraints such as minimum bending radius, curvature of sharp corners, limiting drawing ratio (LDR), Erichsen number and wrinkling limits. With these additions, a functionally complete system is created that can describe the design process of sheet metal forming operations.

The following sections provide a comparative analysis of steel and aluminium sheets, highlighting some of this system's characteristic parameters.

3. Results and Discussion

The most important results are summarised in the following subsections. The first analyses the relationship between the mass of cars and the energy consumption of conventional and electric vehicles, demonstrating that mass is a significant factor in energy usage and CO_2 emissions. This justifies the importance of weight reduction. Subsequent analyses examine the comparison of steel and aluminium sheets in the banana diagram and the strength-density coordinate system, as well as multi-objective optimisation, all from the perspective of weight reduction.

3.1 Recent results in relation to the weight and energy use of cars

The publications presented in the Introduction contain limited amounts of data on the relationship between car type, consumption and emissions. To focus the analysis on vehicle mass, fuel consumption and CO_2 emissions, data on 35 Internal Combustion Engine Vehicle (ICEV) models from 2018 was collected. This was the last year in which a wide range of ICEVs were still available from car manufacturers. The data refers exclusively to Volkswagen products to ensure the cars are as homogeneous as possible in terms of their technical level. Additionally, data on the weight and electric energy consumption (kWh/100 km) of

17 Battery Electric Vehicle (BEV) models from 2024 was collected. The brands examined were Audi, BMW, Chevrolet, Ford, Honda, Hyundai, Jaguar, Kia, Mazda, Mercedes, Nissan, Polestar, Porsche, Renault, Tesla, Volkswagen and Volvo.

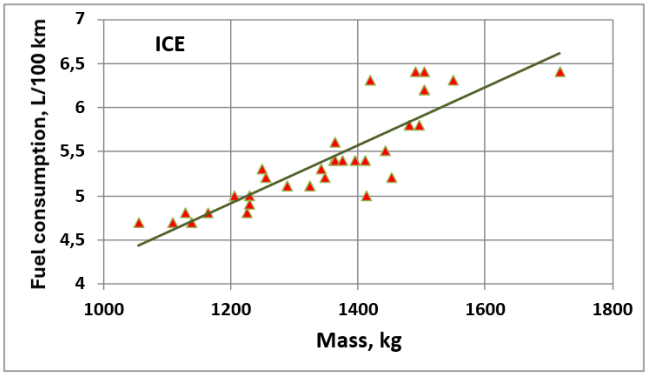

Figure 2. Fuel consumption-mass relations for ICEVs

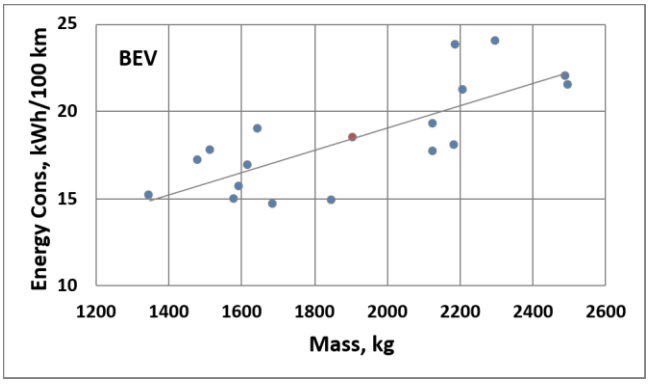

Figure 3. Energy consumption-mass relations for BEVs

Figure 2 shows the fuel consumption values of the ICEV models in litres per 100 km (L/100 km) as a mass function. The diagram shows combined consumption, as it is the most comparable to the energy consumption of BEV models. Figure 3 shows the energy consumption values of BEV models.

Figure 4 shows CO_2 emissions for ICEVs based on manufacturer data, while Figure 5 presents the calculated values for BEV models. According to relevant EU statistics, 1 kWh of electricity is associated with an average of 213 g of CO_2 emissions. Therefore, the energy consumption per 1 km must be multiplied by this value to calculate the gCO_2/km value from electricity generation. However, an additional emission value should be added to this, which is generated during battery production. This can be calculated as 31.5 gCO_2/km over a range of 200,000 km.

The average, minimum and maximum values of the data presented in the figures are shown in Tables 1 and 2. Comparing the two tables shows that BEV models are heavier than ICEV models because the battery significantly increases the weight.

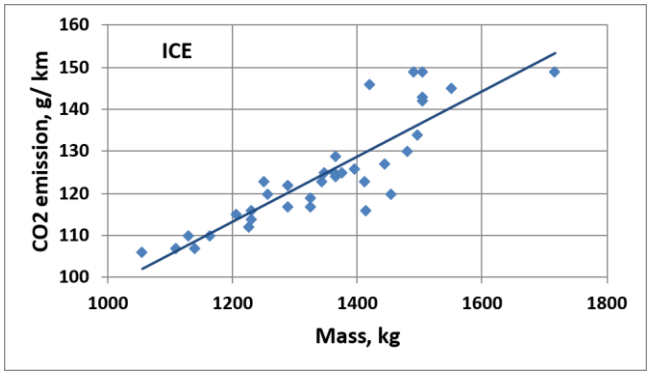

Figure 4. Emission values of ICEVs

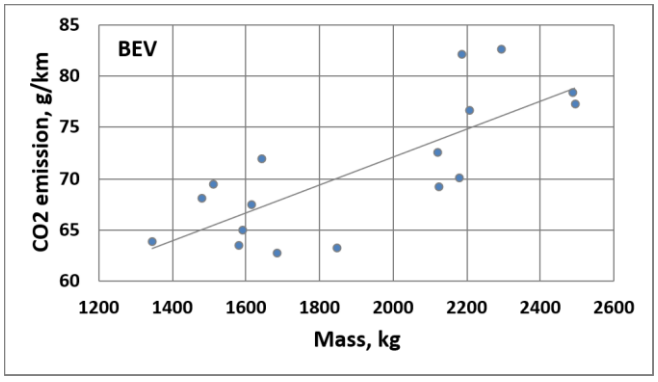

Figure 5. Emission values of BEVs

Table 1. Characteristic figures for ICEVs.

ICEVs	Mass	Fuel Consumption		CO_2 emission
	kg	L/100 km	L/100 km /100 kg	g/100 km /100 kg
Ave	1347	5.4	0.40	927,47
Max	1717	6.4	0.45	1028,17
Min	1055	4.7	0.35	820,95

Table 2. Characteristic figures for BEVs.

BEVs	Mass	Energy Consumption		CO_2 emission
	kg	kWh/100 km	kWh /100 km /100 kg	g/100 km /100 kg
Ave	1906	18.47	0.98	240
Max	2495	24.00	1.18	287
Min	1345	14.70	0.81	197

According to the above calculation, CO_2 emissions are much more favourable for BEVs than for ICEV models if the EU av-

erage value of 213 gCO_2/kWh is considered. However, this advantage does not apply in all countries. In regions where the national energy mix produces up to 900 gCO_2/kWh, charging BEV batteries with such electricity completely negates their emission benefits.

3.2. Comparison of steel and aluminium sheet characteristics

3.3.1. Analysis of the banana diagram

The banana diagram is a traditional classification model for steel sheets that shows the relationship between strength and ductility. The horizontal axis of the diagram shows tensile or yield strength, which is also replaced by specific strength (the strength-to-density ratio), primarily at the initiative of aluminium sheet manufacturers. The latest diagram for steels was published by WorldAutoSteel in 2021 and is now called the Global Formability Chart, as the newly developed extra-high-strength steels have significantly altered its shape. Figure 6 shows an example of this. Figure 7 illustrates a banana diagram for aluminium sheets with specific strength on the horizontal axis. In this comparison, AA5xxx Al-Mg alloys are equivalent to DP series steel sheets and AA6xxx and AA7xxx alloys reach the third generation AHSS category in terms of specific strength. However, the formability of aluminium alloys is significantly lower than that of steels. Magnesium alloys also have good specific strength values, but their formability is poor.

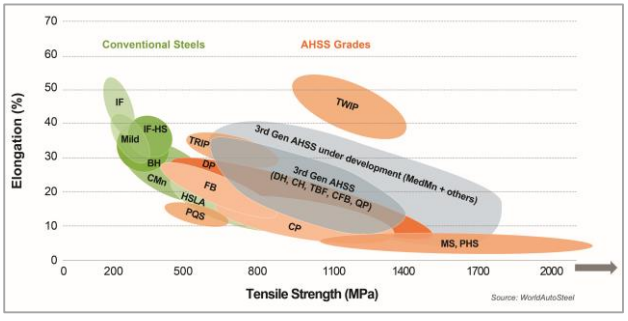

Figure 6. Global Formability Diagram

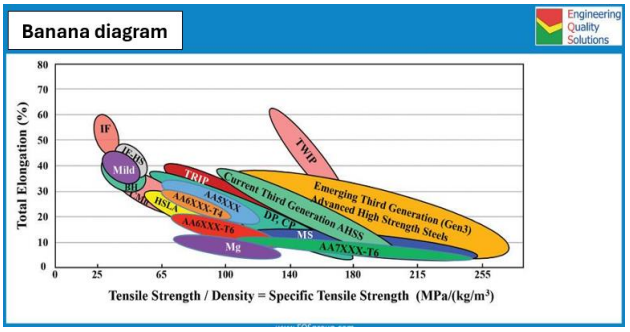

Figure 7. Specific Strength-Total Elongation chart

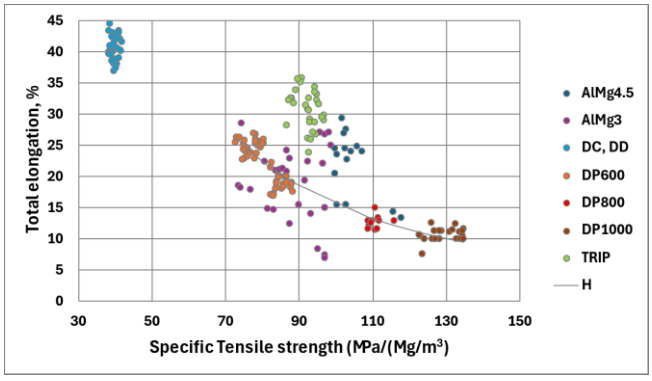

Figure 8. Banana diagram of tested sheets

Comparing these diagrams with the data of our own database, measured points can be seen in Figure 8. The location of the three DP grades roughly corresponds to the relevant data in Figure 6. It is also clear that the AlMg4.5 alloy points are located above the DP points. The AlMg3 points overlap the DP values and the elongation of TRIP700 steel is higher than that of dual-phase steels. The specific strength of the mild steel group (DC and DD) is significantly lower than that of the other sheets, but this is coupled with outstanding elongation. The hyperbola (H) fitted to the DP grades is also shown in the figure.

However, total elongation, which is used as a measure of formability, only characterises part of the forming processes that follow the deformation path close to uniaxial tension, such as deep drawing (see Figure 9). In contrast, a significant proportion of car body panels are formed by biaxial stretching (stretch forming); however, sharp corners and bent edges also require sheets to have special formability properties. These factors are important and should be highlighted, as global formability is well characterised by a banana diagram or forming limit diagram (FLD), but hole expansion tests, edge tension tests, dome tests and Erichsen tests are primarily suitable for classifying local formability. In connection with Figure 1, the difference between global and local formability can be interpreted as follows: global formability is primarily related to the material–process relationship (formability characteristics), while local formability is a characteristic of shape constraints and is closely correlated with manufacturability.

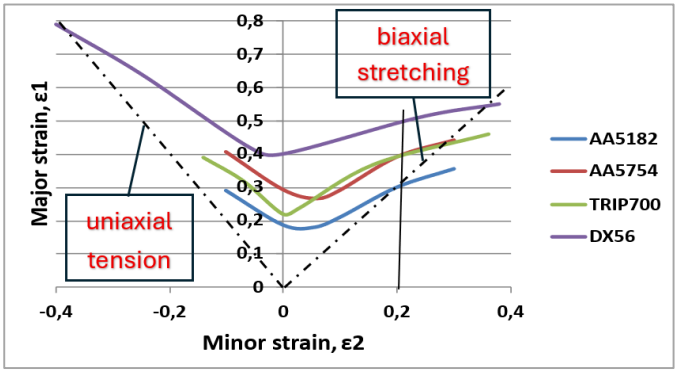

Figure 9. Comparison of FLDs and strain paths

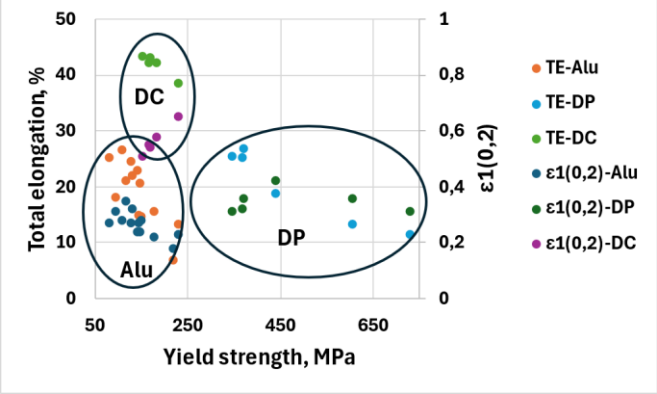

Figure 10. Comparison of total elongation and stretchability of sheets

The right side of the FLD is suitable for modelling stretching related to global formability capability. Therefore, the major strain (ε1(0.2)) at the minor strain ε2=0.2 can be considered an appropriate measure of comparative stretchability (see Figure 9). Figure 10 shows the diagram constructed using the available data from the examined database, illustrating the tensile extension (TE) and the major strain values of ε1(0.2) as a function of yield strength. The distribution of the points suggests that there is only a very weak relationship between the examined quantities.

Figure 11 shows the relationship between the Erichsen number and total elongation for steel sheets, which is used as an indicator of local formability. The trend lines indicate that there is no meaningful correlation between the examined variables. Therefore, tensile extension is not suitable for ranking sheets with strong local formability needs, and according to Figure 10, it can only be used to a limited extent for evaluating the stretch forming abilities of sheets.

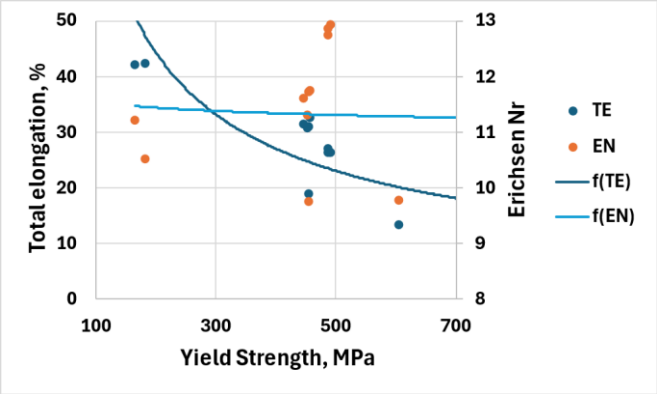

Figure 11. Comparison of total elongation and local formability of sheets

The analysis presented shows that, while the banana chart is a useful tool for illustrating the global correlation between strength and formability, additional information is needed for a detailed analysis of a significant proportion of forming processes.

3.3.2. Comparing steel and aluminium sheets using the strength-density model

A detailed comparative analysis of the application of steel and aluminium in relation to lightweight structures was published earlier [42], analysing the applicability of steel and aluminium sheets based on literature data and public databases. The tests presented here were conducted using our own database, following a similar methodology. According to the Ashby model, a relationship resulting in minimum mass can be established for various load cases, strains, and constraints. In this model, the material properties are represented by 'material indices'. Car body panels are mostly subjected to bending stress. The material indices defined for the strength and stiffness analysis of sheets [9] are as follows:

strength:

$$M_1 = \frac{\rho}{\sigma_y^{1/2}} \quad (1)$$

stiffness

$$M_2 = \frac{\rho}{E^{1/3}} \quad (2)$$

In the above equations, ρ denotes density, σ_y denotes yield strength, and E denotes elastic modulus. Meanwhile, M_1 and M_2 are material indices. Figure 12 shows the points of the examined aluminium and steel sheets, as well as the $M_1 = \rho/\sigma_y^{1/2}$ line according to Eq. (1), in the yield strength–density logarithmic coordinate system. The location of the AlMg3 alloys of lowest strength indicates that they can be comparable with DP600 steel sheets in terms of minimum weight, while the other aluminium alloys result in significantly lower weight. Equation (2) can be used if stiffness is the parameter to be analysed.

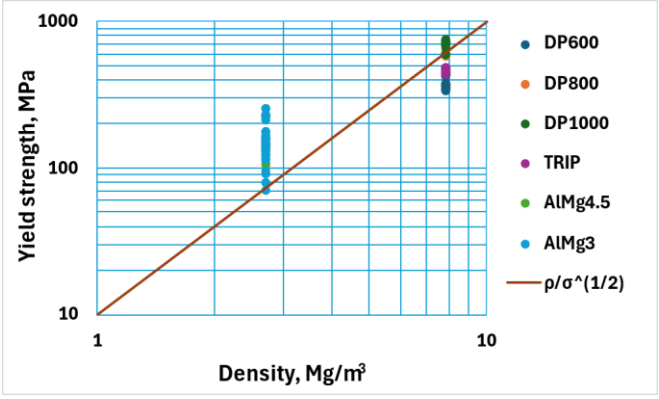

Figure 12. Ashby chart for tested sheets

The relationship between masses is expressed by Eq. (3).

$$\frac{m_i}{m_j} = \frac{\rho_i/\sigma_{yi}^{1/2}}{\rho_j/\sigma_{yj}^{1/2}} \quad (3)$$

This equation can be used to calculate the mass ratios of the main groups of sheets in pairs, forming a matrix shown in Table 3.

Table 3. Mass ratios matrix

	AlMg 3	AlMg 4.5	DC	DP 600	TRIP	DP 800
AlMg 3						
AlMg 4.5	1,04					
DC	0,49	0,47				
DP 600	0,56	0,53	1,13			
TRIP	0,60	0,58	1,22	1,08		
DP 800	0,68	0,66	1,39	1,23	1,14	
DP 1000	0,74	0,71	1,49	1,32	1,22	1,08

The matrix data show that all aluminium alloys produce significant mass reduction compared to steel sheets. To better illustrate the results, the mass ratios of DP1000, DP600 and mild steel (MS) were selected. The resulting bar chart is shown in Figure 13. For example, this shows that the weight of a component made of AlMg4.5 sheet could be 71% of that of a DP1000 component, 53% of a DP600 component, or 43% of an MS component, considering the average yield strength of the data set used. It is known that an average weight reduction of 40% can be achieved using aluminium sheets. The diagram shows that this is realistic, but the actual weight ratio also depends on the strength properties of the original and replacement sheets.

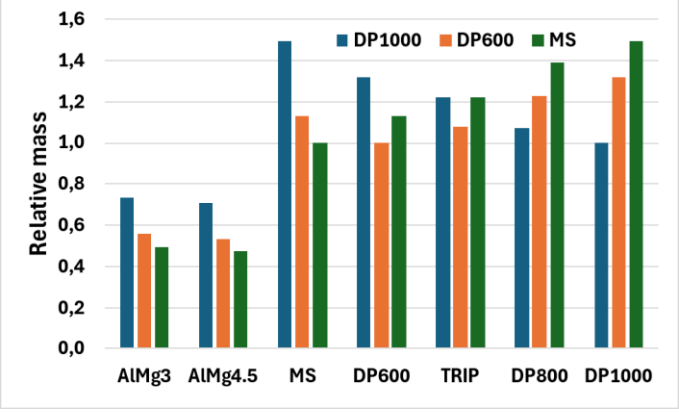

Figure 13. Comparison of mass ratios

3.3.3. Multi-objective optimization of a car body panel

As shown in publications [8, 16-21], multi-objective optimisation is a key application of material selection. Further analysis shows a possible solution for the panel analysed in terms of strength in the previous chapter. Here, the material indices are applied together according to equations (1) and (2), following the method in publication [8]. The shape of the value function (V), as defined by the model, is shown in Eq. (4), where M_1 and M_2 are the performance metrics, as defined in Eqs. (1) and (2), and $\propto_1$ and $\propto_2$ are the exchange constants.

$$V = \propto_1 M_1 + \propto_2 M_2 \quad (4)$$

Taking the defined value of V_d, the relationship between M_1 and M_2 is shown by Eq. (5).

$$M_2 = \frac{V_d}{\propto_2} - \frac{\propto_1}{\propto_2} M_1 \quad (5)$$

The values of the exchange constants can be determined according to the strength/stiffness ratio characteristic of the given part. If the strength requirement is dominant, then α_1 is higher; in other cases, the stiffness exchange constant may be more significant. In general, the strength and stiffness requirements are equal for floor panels. In the crash zone, stiffness is more important, while for doors and the A and B pillars, strength is more favourable. Taking these factors into account, the $\propto_1$ and $\propto_2$ exchange constants can be selected according to the given component. The function defined in this way produces a straight line in the M_1-M_2 coordinate system (see Eq. 5), the slope of which is $-\propto_1/\propto_2$. Its position depends on the value of V_d. These lines are shown in Figure 14, with the dashed lines representing the slopes SL(-4), SL(-2) and SL(-1) starting from the (0;1.4) point. To emphasise strength, values of $\propto_1 = 0.8$ and $\propto_2 = 0.2$ might be a suitable choice for the exchange constants. Using these values, other parallel lines with SL (-4) are displayed in the chart together with the average yield strength of the sheets in the database on the M1 axis. The points on the M2 axis are located at the same height because the elastic modulus (E) is approximately the same for each group of materials. This chart shows a different arrangement of materials to that in publication [8], but the evaluation and ranking of materials may be similar.

From the diagram, it can be concluded that, when the chosen exchange constant values are applied, magnesium sheets would be the most favourable, followed by titanium and aluminium alloys, with steel sheets being the least favourable. Of course, these statements apply only to the given exchange constant values; in the case of other parts, the chosen coefficients can change the order.

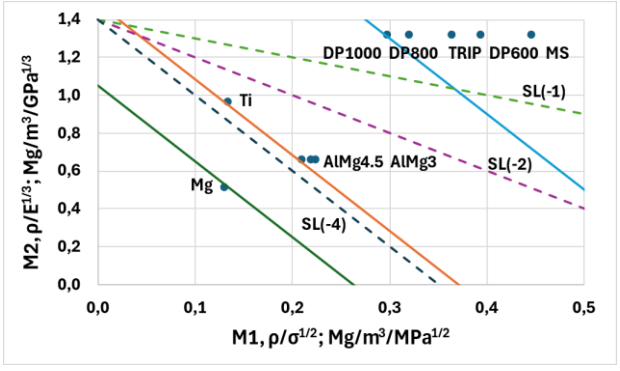

Figure 14. Value functions plotted with material performance metrics

4. Conclusions

The use of lightweight materials in vehicle production is a key trend in the automotive industry, driven by the need for efficiency, sustainability, and improved performance. The advanced high-strength steels and AlMg aluminium alloys were analysed as key materials. For this analysis, a sheet-specific form of the Ashby concept was developed, supplementing the Material-Shape-Process parameters with three additional databases: Design parameters, Formability characteristics and Shape constraints.

First, the impact of weight reduction on energy consumption was examined using data from internal combustion engine and battery electric vehicles. The analysis clearly shows that

- a 100 kg mass reduction results in a ~6.4% decrease in fuel consumption for ICEVs and a 4.2% energy saving for BEVs, with the same emission reduction being achieved.
- the average energy usage is ~1.1 kWh/100 km/100 kg for ICEVs and ~1 kWh/100 km/100 kg for BEVs.

Based on the banana chart created from our own database of measurements, it was observed that

- data points for different steel sheets follow the global trends reported in previous publications, albeit with a larger scatter,
- evaluation of the diagram showed that this data only partially characterises formability and that consideration of further global and local formability parameters is needed when designing sheet forming operations.

The major strain at 0.2 minor strain within the biaxial range of the forming limit diagram and the Erichsen number were compared with tensile elongation in the banana diagram. It could be concluded that:

- these characteristics only follow the trend defined in the banana diagram to a limited extent,
- a parameter set according to the extended Ashby concept is needed to characterise the complex forming process.

The multi-objective optimisation of the strength and stiffness parameters of the tested sheets resulted in a chart of specific material indices, with the limited material groups arranged horizontally according to elastic modulus. Analysing a possible load case for the sheets established the order of the sheet groups.

Acknowledgment

The research presented in this paper was funded by the National Security Subprogram at the Széchenyi István University (TKP2021-NVA-23).

Conflict of Interest Statement

The author declares that there is no conflict of interest in the study.

References

[1] Harvey D. Rethinking electric vehicle subsidies, rediscovering energy efficiency. Energy Policy 2020;146:111760. https://doi.org/10.1016/j.enpol.2020.111760

[2] Wenlonga S, Xiaokaia, Lub C. W. Analysis of Energy Saving and Emission Reduction of Vehicles Using Light Weight Materials. Energy Procedia. 2016;88:889-893. https//:doi.org/10.1016/j.egypro.2016.06.106

[3] Taşdemir V. Finite Element Analysis of Bending Zone Damage and Springback Behavior After V Bending Process of AA5754 Alloy. International Journal of Automotive Science and Technology. 2025; 9 (2): 241-248. https://doi.org/10.30939/ijastech..1624367

[4] Zhang W, Xu J. Advanced lightweight materials for Automobiles: A review. Mater. Des. 2022;221:110994. https://doi.org/10.1016/j.matdes.2022.110994

[5] Srinivasa K. Advancements in lightweight materials for automobile design: impact on fuel efficiency and safety. World Journal of Advanced Research and Reviews, 2019;02(01):063-069. https://doi.org/10.30574/wjarr.2019.2.1.0118

[6] Albińana J.C, Vila C. A framework for concurrent material and process selection during conceptual product design stages. Materials and Design 2012;41:433–446. https://doi.org/10.1016/j.matdes.2012.05.016

[7] Ashby M.F. Materials Selection in Mechanical Design. Pergamon Press. 1992

[8] Ashby, M.F. Multi-Objective Optimization in Material Design and Selection. Acta Materiala, 2000;48:359–369. https://doi.org/10.1016/S1359-6454(99)00304-3

[9] Ashby M.F, Brechet Y.J.M, Cebona D, Salvoc L. Selection strategies for materials and processes. Materials and Design 2004;25:51–67. https://doi.org/10.1016/S0261-3069(03)00159-6

[10] Ashby M.F, Johnson K. Materials and Design: The Art and Science of Material Selection in Product Design, 2nd ed.; Butterworth Heinemann: Oxford, UK. 2013

[11] Okafor C. E, Oghenemaero O. O, Chukwuebuka M, Isaac O. O. Adaptive design of a universal automotive ball joint separating device. Transportation Engineering 2020;2:100010. https://doi.org/10.1016/j.treng.2020.100010

[12] Lovatt A.M, Shercliff H.R. Manufacturing process selection in engineering design. Part 1: the role of process selection. Materials and Design 1998;19:205-215. https://doi.org/10.1016/S0261-3069(98)00038-7

[13] Amany A, Pasini D. Material and shape selection for stiff beams under non-uniform flexure. Materials and Design 2009;30:1110–1117. https://doi.org/10.1016/j.matdes.2008.06.029

[14] Pasini D. Shape transformers for material and shape selection. Materials and Design 2007;28(7):2071–9. https://doi.org/10.1016/j.matdes.2006.05.028

[15] Risaliti E, Gabriele A, Del Pero F, Citti P. Innovative Model for Material Selection Within the Automotive Lightweight Eco-

Design Field. Eng. Proc. 2025;85:20. https://doi.org/10.3390/engproc2025085020

[16] Rao R.V, Patel B.K. A subjective and objective integrated multiple attribute decision making method for material selection. Materials and Design 2010;31:4738–4747. doi:10.1016/j.matdes.2010.05.014

[17] Kumar R, Jagadish A. R. Selection of Material for Optimal Design using Multi-Criteria Decision Making. Procedia Materials Science 2014;6:590-596. https://doi.org/10.1016/j.mspro.2014.07.073

[18] Sen B, Bhattacharjee P, Mandal U. K. A comparative study of some prominent multi criteria decision making methods for connecting rod material selection. Perspectives in Science 2016;8:547-549. http://dx.doi.org/10.1016/j.pisc.2016.06.016

[19] Lu H, Behbahani S, Mac X, Iseley T. A multi-objective optimizer-based model for predicting composite material properties. Construction and Building Materials 2021;284:122746. https://doi.org/10.1016/j.conbuildmat.2021.122746

[20] Hanaoka, K. Comparison of conceptually different multi-objective Bayesian optimization methods for material design problems. Materials Today Communications 2022;31:103440. https://doi.org/10.1016/j.mtcomm.2022.103440

[21] Conrad F, Stöcker J.P, Signorini C, Salgado I, de P. Wiemer H, Kaliske M, Ihlenfeldt S. Exploring design space: Machine learning for multi-objective materials design optimization with enhanced evaluation strategies. Computational Materials Science 2025;246:113432. https://doi.org/10.1016/j.commatsci.2024.113432

[22] Palencia J. C. G, Furubayashi T, Nakata T. Energy use and CO2 emissions reduction potential in passenger car fleet using zero emission vehicles and lightweight materials. Energy 2012;48:548-565. http://dx.doi.org/10.1016/j.energy.2012.09.041

[23] Simões C. L, Figueiriedo de Sá R, Ribeiro C. J, Bernardo P, Pontes A. J, Bernardo C.A. Environmental and economic performance of a car component: assessing new materials, processes and designs. Journal of Cleaner Production 2016;118:105-117. http://dx.doi.org/10.1016/j.jclepro.2015.12.101

[24] Hao H, Geng Y, Sarkis J. Carbon footprint of global passenger cars: Scenarios through 2050. Energy 2016;101:121-131. https://doi.org/10.1016/j.energy.2016.01.089

[25] Shen J, Zhang Q, Tian S. Impact of the vehicle lightweighting and electrification on the trend of carbon emissions from automotive materials. Journal of Cleaner Production, 2025; https://doi.org/10.1016/j.jclepro.2025.145677

[26] Poulikidou S, Schneider C, Björklund A, Kazemahvazi S, Wennhage P, Zenkert D. A material selection approach to evaluate material substitution for minimizing the life cycle environmental impact of vehicles. Materials & Design 2015;83:704–712. http://dx.doi.org/10.1016/j.matdes.2015.06.079

[27] Ain O, Khalil H. B, El-Maraghy M, Marzouk M. Generative design and multi-objective optimization for enhanced building thermal performance. Case Studies in Thermal Engineering 2025;73:106621. https://doi.org/10.1016/j.csite.2025.106621

[28] Souvanhnakhoomman S, Chua, A. A comprehensive review of generative design applications in unmanned aerial vehicles. ASEAN Engineering Journal March 2025. doi: 10.11113/aej.v15.21286

[29] Chen Y, Qin Z, Sun L, Wu J, Ai W, Chao J, Li H, Li J. GDT Framework: Integrating Generative Design and Design Thinking for Sustainable Development in the AI Era. Sustainability 2025;17:372. https://doi.org/10.3390/su17010372

[30] Menon D, Ranganathan R. A Generative Approach to Materials Discovery, Design, and Optimization. ACS Omega 2022;7:25958−25973. https://doi.org/10.1021/acsomega.2c03264

[31] Sreenivasan A, Suresh M. Design thinking and artificial intelligence: A systematic literature review exploring synergies. International Journal of Innovation Studies 2024;8:297–312. https://doi.org/10.1016/j.ijis.2024.05.001

[32] Papadimitriou I, Gialampoukidis I, Vrochidis S, Kompatsiaris I. AI methods in materials design, discovery and manufacturing: A review. Computational Materials Science 2024;235:112793. https://doi.org/10.1016/j.commatsci.2024.112793

[33] Chandrasekhar A. Sridhara S. & Suresh, K. Integrating material selection with design optimization via neural networks. Engineering with Computers 2022;38:4715–4730. https://doi.org/10.1007/s00366-022-01736-0

[34] Delogu M, Zanchi L, Dattilo C.A, Pierini M. Innovative composites and hybrid materials for electric vehicles lightweight design in a sustainability perspective. Materials Today Communications 2017;13:192–209. http://dx.doi.org/10.1016/j.mtcomm.2017.09.012

[35] Bader B, Altacha J, Türcka E, Vietor, T. Approach for assessment of suitable automotive component ranges for the application of multi material design. Procedia CIRP 2020;91:188–193. doi: 10.1016/j.procir.2020.03.099

[36] Hu J, Thomas G. Evolving the ‘‘Banana Chart’’: Temperature and Strain Rate Effects on Tensile Properties of New-Generation Advanced High-Strength Steels. JOM, 2021;73:11. https://doi.org/10.1007/s11837-021-04900-x

[37] Billur E, Karabulut S, Yılmaz I. Ö, Erzincanoğlu S, Çelik H, Altınok E, Başer T. Mechanical Properties of Trip Aided Bainitic Ferrite (TBF) Steels in Production and Service Conditions. Hittite Journal of Science and Engineering, 2018;5(3):231-237. DOI: 10.17350/HJSE19030000100

[38] Suwanpinij P. The Synchrotron Radiation for Steel Research. Advances in Materials Science and Engineering 2016; ID 2479345, 6 pages. http://dx.doi.org/10.1155/2016/2479345

[39] Yassine M, Tisza M. Formability Investigations of Advanced High Strength Steels. MultiScience - XXXII. microCAD International Multidisciplinary Scientific Conference. 2018; Miskolc, Hungary.
[40] Banabic D. Sheet Metal Forming Processes. Springer-Verlag Berlin Heidelberg. 2010
[41] Banabic D, Barlat F, Cazacu O et al. Advances in anisotropy of plastic behaviour and formability of sheet metals. Int J Mater Form 2020;13:749–787. https://doi.org/10.1007/s12289-020-01580-x
[42] Tisza, M. Czinege, I. (2018). Comparative study of the application of steels and aluminium in lightweight production of automotive parts, International Journal of Lightweight Materials and Manufacture, 1-10. https://doi.org/10.1016/j.ijlmm.2018.09.001